Carbohydrate Polymers 90 (2012) 644–649

Contents lists available at SciVerse ScienceDirect

Carbohydrate Polymers

journal homepage: www.elsevier.com/locate/carbpol

Colloidal stability of negatively charged cellulose nanocrystalline in aqueous systems

Linxin Zhong[a], Shiyu Fu[b,*], Xinwen Peng[b], Huaiyu Zhan[b], Runcang Sun[a]

[a] College of Material Science and Technology, Beijing Forestry University, Beijing, China
[b] State Key Laboratory of Pulp and Paper Engineering, South China University of Technology, Guangzhou 510640, China

ARTICLE INFO

Article history:
Received 21 March 2012
Received in revised form 18 May 2012
Accepted 24 May 2012
Available online 1 June 2012

Keywords:
Cellulose nanocrystalline
Colloidal stability
Electrolyte
Zeta potential

ABSTRACT

Colloidal stability of negatively charged cellulose nanocrystalline (CNC) in the presence of inorganic and organic electrolytes was investigated by means of dynamic light scattering and atomic force microscopy. CNC could be well dispersed in distilled water due to the electrostatic repulsion among negatively charged sulfate ester groups. Increasing the concentration of inorganic cation ions (Na^+ and Ca^{2+}) resulted in CNC aggregation. CNC in divalent cation ion Ca^{2+} solution exhibited less stability than that in monovalent cation ion Na^+ solution. Organic low-molecular-weight electrolyte sodium dodecyl sulfate (SDS) favored the stability of CNC suspension, whereas organic high-molecular-weight electrolyte sodium carboxymethyl cellulose (CMC) induced CNC particle aggregation due to intermolecular bridging interaction or entanglement. Cationic polyacrylamide (CPAM) caused a serious aggregation of CNC particles even at low concentration of CPAM. At low ionic strength (Na^+, 1 mM), CNC were stable in aqueous solution at the pH range of 2–11.

1. Introduction

Cellulose nanocrystalline (CNC) has received a great deal of attention in the last two decades due to its unique self-assembly, liquid crystalline behaviors (Cranston & Gray, 2006; Habibi, Lucia, & Rojas, 2010), optical properties (Shopsowitz, Qi, Hamad, & MacLachlan, 2010), excellent mechanical strength (Sturcova, Davies, & Eichhorn, 2005), and potential applications as a novel reinforcement and nanofiller in nanocomposites (George & Bawa, 2010; Ljungberg et al., 2005; Samir, Alloin, & Dufresne, 2005). CNC particles are usually obtained from native cellulose sources by controlled acid hydrolysis (Elazzouzi-Hafraoui et al., 2008). The use of sulfuric acid has been shown to produce CNC with sulfate ester groups on the nanocrystal surface, resulting in electrostatically stabilized aqueous suspensions of CNC (Dong & Gray, 1997). In a dilute aqueous system, CNC particles are well dispersed and orient randomly due to electrostatic repulsion among negatively charged sulfate ester groups. Above a critical CNC concentration, however, anisometric rodlike shape and negative surface charge of CNC will result in an upper isotropic phase and a lower ordered phase in aqueous system (Beck-Candanedo, Roman, & Gray, 2005; De Souza Lima & Borsali, 2002; Dong, Kimura, Revol, & Gray, 1996; Revol, Bradford, Giasson, Marchessault, & Gray, 1992).

The zeta potential plays an important role in determining the colloidal stability of nano particles in aqueous solutions (Leong & Ong, 2003; Wang & Wei, 2001). The influences of electrolytes on the phase separation and chiral nematic texture of CNC had been reported in literatures. It was found that the isotropic-to-chiral nematic phase equilibrium was sensitive to the nature of the counterions present in the suspension. Adding electrolyte (NaCl) induced a decrease in the chiral nematic pitch and an increase in the chiral twist power (Hirai, Inui, Horii, & Tsuji, 2009). A decrease in double layer thickness would increase the chiral interactions between the crystallites (Dong et al., 1996). For inorganic counterions, the critical concentration for ordered phase formation increased with the increase of ionic strength (De Souza Lima & Borsali, 2004; Dong, Revol, & Gray, 1998). For organic counterions, the critical concentration in general increased with increasing counterion size, suggesting that the phase equilibrium was governed by a balance between hydrophobic attraction and steric repulsion forces (Dong & Gray, 1997). Increasing Na^+ concentration resulted in the decrease in the zeta potential of CNC, which led to the instability of CNC suspension (Araki & Kuga, 2001; Boluk, Lahiji, Zhao, & McDermott, 2011). However, the electrokinetic behaviors of CNC in electrolyte solutions are not up to now well understood. In this work, the influences of electrolyte composition and pH on the colloidal stability of CNC suspension were investigated in detail by means of dynamic light scattering (DLS) and atomic force microscopy (AFM). This work showed some interesting findings about the CNC suspension, and allowed us to better understand

---

* Corresponding author. Tel.: +86 20 87112453; fax: +86 20 22236078.
E-mail address: shyfu@scut.edu.cn (S. Fu).

0144-8617/$ – see front matter © 2012 Elsevier Ltd. All rights reserved.
http://dx.doi.org/10.1016/j.carbpol.2012.05.091

the colloidal stability of CNC in aqueous systems, which is very important for preparation of CNC-based materials.

2. Experiment

2.1. Materials

Commercial cotton linter with a particle size of 200 mesh was purchased from Xuanyuan Machinery Inc. (Shandong, China). The α-cellulose content was over 98% and the ash content was less than 0.06%. The cellulose was used without any further purification. Its viscosity-average molecular weight ($M\eta$) was measured to be 4.3×10^4. Sulfuric acid (98%, w/w), NaCl, $CaCl_2$ and sodium carboxymethyl cellulose (CMC) were purchased from Shanghai Chemical Reagent Corp., China. Sodium dodecyl sulfate (SDS) and cationic polyacrylamide (CPAM) were purchased from Guangzhou Chemical Reagent Factory, China.

2.2. CNC preparation

CNC particles used in this work were prepared by acid hydrolysis of cotton linter. Typically, cotton linter (20 g) was mixed with sulfuric acid (200 mL, 64 wt%) and stirred at 45 °C for 2 h, and then diluted with deionized water to stop the reaction. The acid was removed by centrifugation and prolonged dialysis with deionized water. Finally, the suspension was further dispersed in an ultrasonic bath to achieve a stable colloidal suspension.

2.3. Zeta potential and size of CNC suspensions with different electrolytes and pH

All experiments were carried out in dilute CNC suspension (0.15 wt%) where CNC particles randomly oriented. The dynamic light scattering (DLS, Zeta sizer Nano ZS, Malvern instrument) was used to evaluate the colloidal stability (zeta potential and size) of CNC suspensions as functions of ionic strength, electrolyte composition and pH. The zeta potential and size of the CNC particles in electrolyte solutions were measured over a range of electrolyte concentration (0–50 mM) at 25 °C. Electrolytes NaCl and $CaCl_2$ (Shanghai Chemical Reagent Corp., China) were applied as inorganic electrolytes. CPAM, CMC, and SDS were used as organic electrolytes. All reagents were analytical grade and were used without further purification.

The influence of pH (2–12) on the colloidal stability of CNC suspension was also investigated. The stock CNC dispersion was mixed with appropriate quantities of HCl, NaCl and NaOH solutions to achieve a required pH. In the pH range of 2–11, the ionic strength (Na^+) of CNC suspensions was 1 mM, while in the suspension of pH 12 the ionic strength was 10 mM. All of the CNC suspensions were previously ultrasonified for 5 min in an ultrasound bath to disrupt any weakly formed aggregates before adding any electrolyte, and then stood for 5 min before measurement. All suspensions were prepared in deionized water. Data are representative of at least three experiments varied by less than 5% in all the cases studied.

2.4. AFM analysis

AFM was performed using a Nanoscope III (Veeco Co. Ltd., USA). The samples for AFM were prepared by dropping CNC suspension onto the mica surface and then air dried the sample at ambient temperature. All of the images were recorded in tapping mode in air using silicon cantilevers. The scale in all testing was 2.0 μm × 2.0 μm.

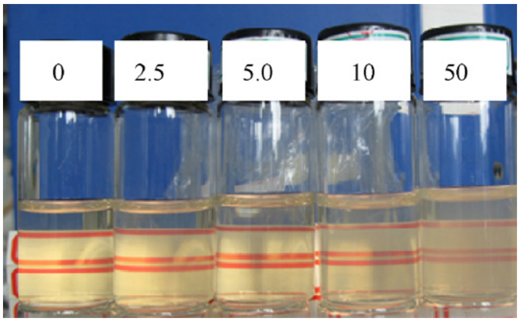

Fig. 1. Aqueous CNC suspensions with ionic strength (Na^+) of 0.0, 2.5, 5.0, 10.0, and 50.0 mM.

3. Results and discussion

3.1. Inorganic electrolytes

In a dilute system, the colloidal stability of charged particles is controlled by the electrostatic interactions. Particles who have an absolute value of zeta potential of more than 30 mV may keep their suspensions stable; otherwise the particles tend to approach each other with the result of CNC aggregation. For charged particles, the electrostatic contribution to the interparticle forces depends on the ionic strength of the system. Counterions will associate with the charged particles and thus play a very important role in determining the interparticle forces. Since sulfate ester groups are introduced onto the CNC surface by sulfuric acid hydrolysis, electrostatically stabilized CNC suspension can be obtained in aqueous solution (Dong et al., 1996). In this work, NaCl, $CaCl_2$, SDS, CMC and CPAM were chosen as inorganic and organic electrolytes to investigate the influences of ionic strength and electrolyte composition on the colloidal stability of CNC particles in aqueous solution.

In the absence of electrolyte (at the smallest ionic strength that could be reached), CNC suspension was clear and transparent (Fig. 1), which indicates a good dispersion and colloidal stability of CNC in aqueous solution due to the negative charge repulsion among CNC particles. AFM image revealed that the CNC particles were rodlike with diameter of 100–270 nm long and 40–80 nm wide (Fig. 2). The average zeta potential and size of CNC determined by DLS were about 118 nm and −52.6 mV (Fig. 3a). Clearly, strong electrostatic repulsion among CNC particles gave rise to a stable CNC suspension.

At a low ionic strength (2.5 or 5.0 mM Na^+), CNC suspension was still clear and transparent, and no particle aggregation or turbid suspension could be observed (Fig. 1). The absolute value of zeta potential decreased from 38.6 to 33.4 mV as the ionic strength increased from 2.5 to 5.0 mM, but there was no difference in size between the two CNC suspensions, as illustrated in Fig. 3a. The decrease in zeta potential is due to the electrostatic screening effect of cation counterion Na^+. Double layer principles imply that counterions in solution shield the surface charges of particles, which thus reduces the absolute value of zeta potential and the electrostatic repulsion. An absolute value of zeta potential of more than 30 mV is sufficient to produce strong electrostatic repulsion and thus a stable CNC colloid at low Na^+ concentration ($\leq$5.0 mM).

As the ionic strength increased to 10 mM and to 50 mM, the zeta potential became less negative (−25.8 and −16.5 mV), and the particle size increased to 151 nm (10 mM) and 980 nm (50 mM). This indicates that charge screening effect was prominent and led to particle aggregation, therefore turbid suspensions were observed at ionic strength of 10 and 50 mM (Fig. 1). AFM also revealed that 10 mM Na^+ started to cause particle aggregation (Fig. 2), which well agrees with the results obtained from DLS. When the absolute value of zeta potential is less than 30 mV, the

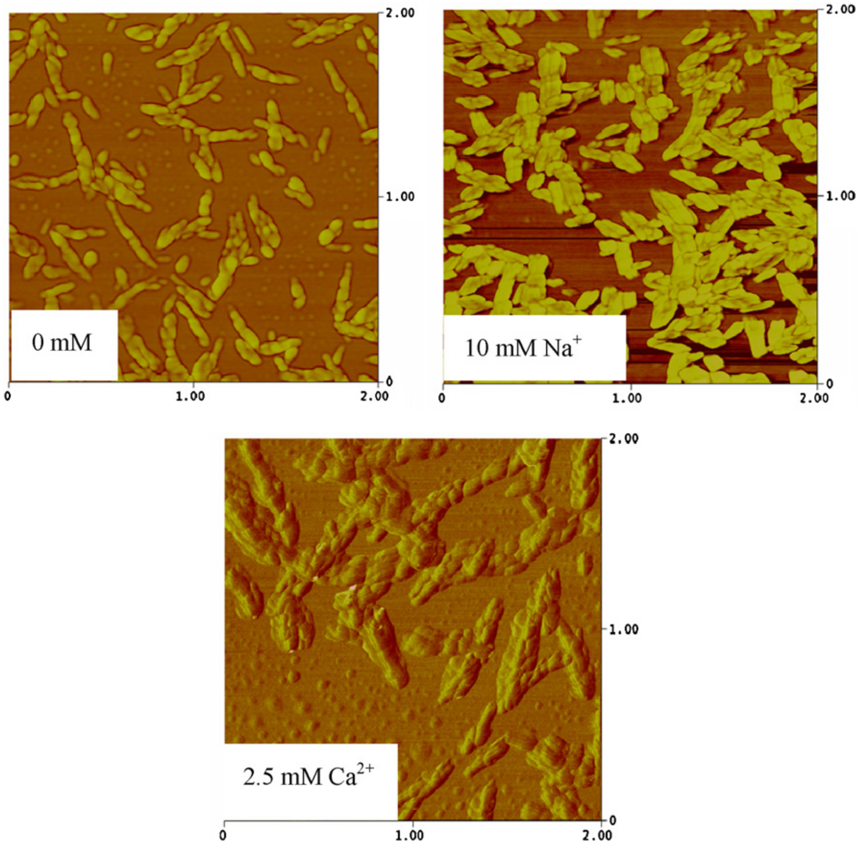

Fig. 2. AFM images of CNC suspensions in inorganic electrolyte solutions. The scanning scale is 2 μm × 2 μm.

van der Waals force dominates the electrostatic repulsion and thus the charged particles tend to aggregate. Boluk et al. (2011) also found that CNC suspension was kinetically unstable as NaCl concentration is higher than 10 mM. It was further observed that a higher ionic strength produced a more turbid solution, and the phase separation was fast at ionic strength of 50 mM (Borgström, Egermayer, Sparrman, Quist, & Piculell, 1998).

The phase equilibrium of CNC is very sensitive to the added electrolyte. The influence of electrolyte on the liquid crystal phase of CNC suspension had been reported in literatures. Araki and Kuga (2001) reported that addition of trace electrolyte (0.1 mM NaCl) led to the formation of the chiral nematic phase. The presence of electrolyte (1.0 mM) decreased the volume of the lower anisotropic phase significantly for a 1.58 wt% cellulose suspension. Dong et al. (Dong et al., 1996) reported that the volume fraction of the chiral nematic phase of cotton cellulose decreased from 0.56 to 0.05 with an increase in the NaCl concentration from 0.0 to 2.4 mM. The chiral nematic pitch of the anisotropic phase decreased with the added electrolyte concentration. Apparently, a decrease in double layer thickness increased the chiral interactions between the crystallites (Dong et al., 1996). In this work, the dilute CNC suspension showed their colloidal instability at Na^+ concentration of more than 5 mM, which indicates that a dilute CNC suspension is less sensitive to counterion than liquid crystal concentration, which is mainly due to the weaker interaction between particles at low CNC concentration.

The influence of the divalent counterion Ca^{2+} on the colloidal stability of negatively charged CNC is presented in Fig. 3b. As Ca^{2+} concentration increased, the zeta potential of CNC became less negative due to electrostatic screening effect of counterion. At low Ca^{2+} concentrations ($\leq$1 mM), the absolute value of zeta potential was more than 30 mV, thus repulsive force dominated and little aggregation occurred to CNC particles, which was also indicated by the CNC particle size of 116–119 nm in Fig. 3b. At higher Ca^{2+} concentrations (2.5–5.0 mM), the absolute value of zeta potential was less than 30 mV −15.6 to −7.8 mV), which resulted in that the attractive van der Waals force dominated over the repulsive force, and therefore, particles tended to aggregate due to the decreasing repulsion barrier, as indicated by the CNC size of 325 nm (2.5 mM) and 752 nm (5.0 mM). A representative AFM image of CNC aggregations at Ca^{2+} concentration of 2.5 mM is presented in Fig. 2. As compared with the samples without and with Na^+ (10 mM) (Fig. 2), CNC suspension with Ca^{2+} (2.5 mM) more easily tended to aggregate and the size of the CNC aggregation was much larger, suggesting an instable colloid system.

For both NaCl and $CaCl_2$ solutions, the zeta potential of CNC became less negative with the increasing ionic concentration, which is commonly observed with most colloidal particles in aqueous solution. The zeta potential of CNC, however, was less sensitive to NaCl concentration than $CaCl_2$ over the same ionic concentration range. When 10 mM Na^+ started to cause CNC aggregation in NaCl solution, only 2.5 mM Ca^{2+} could lead to CNC aggregation in $CaCl_2$ solution. At ionic strength of 5.0 mM, the zeta potential and particle size of CNC suspension with Ca^{2+} was more turbid than that one with Na^+, which is displayed in Fig. 4. This difference is attributed to the stronger screening effect of divalent counterion Ca^{2+} than that of monovalent counterion Na^+. A specific adsorption of Ca^{2+} on the surface of CNC particles might also occur (Brant, Lecoanet, Hotze, & Wiesner, 2005).

3.2. Organic electrolytes

It was found that organic electrolytes could induce the phase separation of anisotropic CNC suspension (Beck-Candanedo, Viet, & Gray, 2006; Edgar & Gray, 2002). In this study, SDS, CMC and CPAM

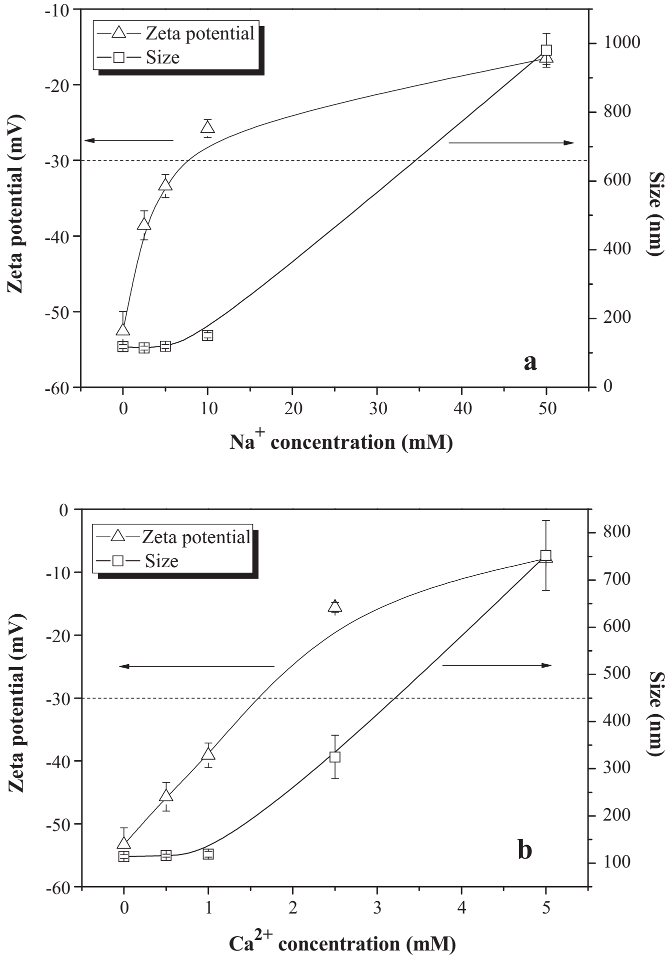

Fig. 3. Zeta potential and size of CNC as functions of Na$^+$ (a) and Ca^{2+} (b) concentrations.

were chosen as anionic and cationic electrolytes to investigate the influences of organic electrolytes on the colloidal stability of CNC suspension.

Fig. 5a shows the influence of SDS concentration on the zeta potential and size of CNC. At low concentrations ($\leq$1.0 g/L), SDS showed little influence on the zeta potential, while higher SDS concentrations resulted in zeta potential becoming more negative. The zeta potentials are −56.9 mV, −76.9 mV and −79.5 mV for CNC at SDS concentrations of 1.0 g/L, 5.0 g/L and 15.0 g/L, respectively. The nanoparticle size showed little difference (116–119 nm) at SDS concentration range of 0.0–5.0 g/L, and then it slightly decreased to 105 nm at SDS concentration of 15.0 g/L. Because both SDS and CNC are negatively charged, the electrostatic repulsion led to a low absorption of SDS on CNC surface, especially at low SDS concentrations, which resulted in minor change in zeta potential and size of CNC. At high concentrations, more SDS presented around CNC particles and therefore made the zeta potential more negative. In addition, the presence of SDS among CNC particles might also act as a steric stabilizer to stabilize the nanoparticles. In this case, entanglement of SDS chains would not happen because of the low molecular weight of anionic SDS. These effects allowed a more stable CNC suspension, which can be further confirmed by the well dispersed CNC particles (Fig. 6) and the transparent suspension (Fig. 7).

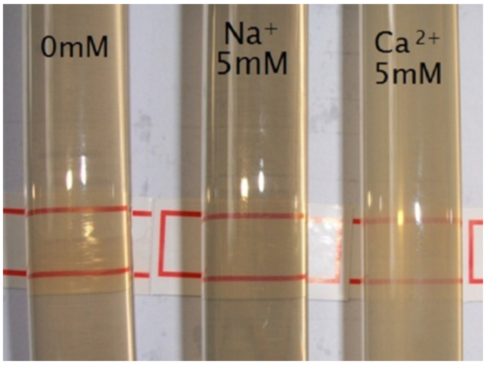

Fig. 4. Colloidal stability of CNC in inorganic electrolyte solutions.

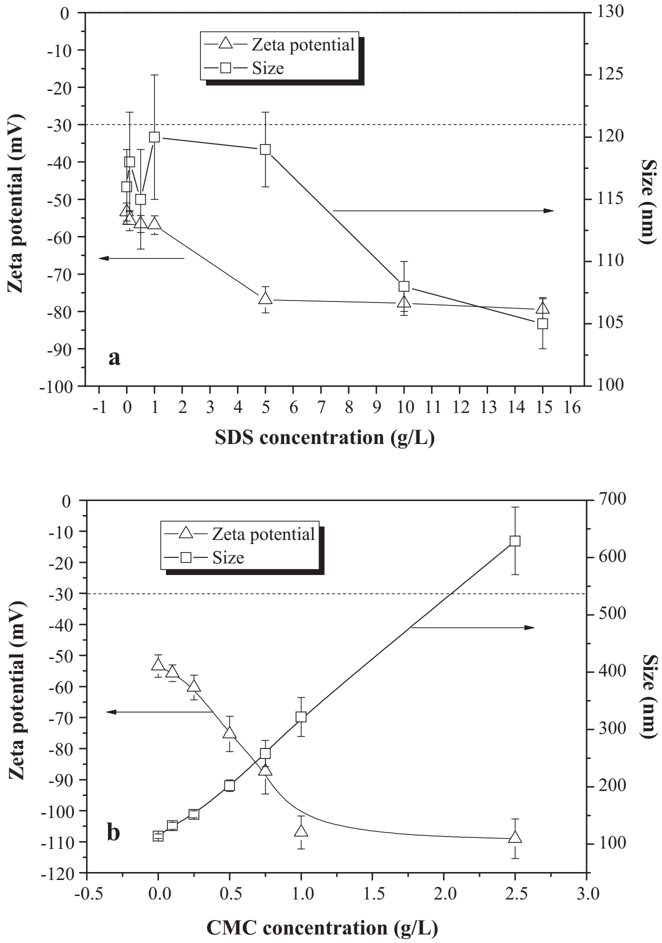

Fig. 5. Zeta potential and size of CNC as functions of SDS (a) and CMC (b) concentrations.

Fig. 5b shows the influence of CMC on the colloidal stability of CNC suspension. The zeta potential became more negative with the increase of CMC concentration, whereas the particle size increased. CNC size slightly decreased with the increase of the absolute value of zeta potential in SDS solution (Fig. 5a), whereas CNC size increased with the increasing absolute value of zeta potential in CMC solution, which can also be confirmed by the larger CNC aggregates in Fig. 6 and the turbid suspension in Fig. 7. CMC is a high-molecular-weight anionic electrolyte; the long molecular chain may cause bridging interaction or intermolecular entanglement, and thus brought about serious aggregation of CNC.

It was also observed that only 0.5 g/L CPAM started to cause CNC aggregation, as shown in Fig. 7. In this case, cation polyelectrolyte strongly absorbed onto the negatively charged CNC surface, causing electrostatic screening effect (Edgar & Gray, 2002). More importantly, bridging interaction or intermolecular

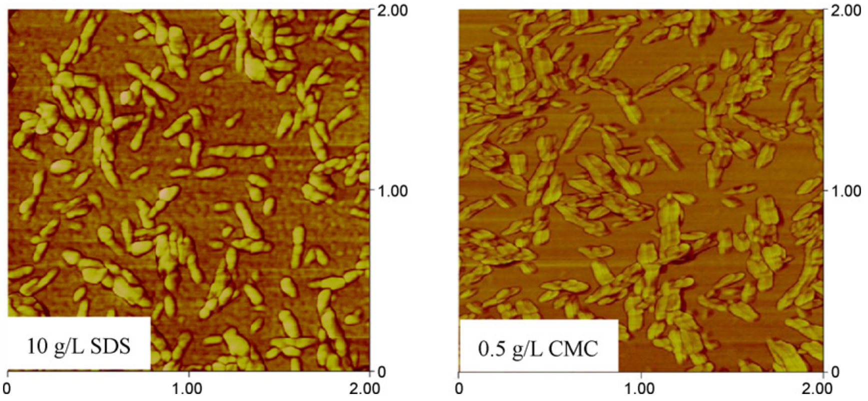

Fig. 6. AFM images of CNC suspensions in organic electrolyte solutions. The scanning scale is 2 μm × 2 μm.

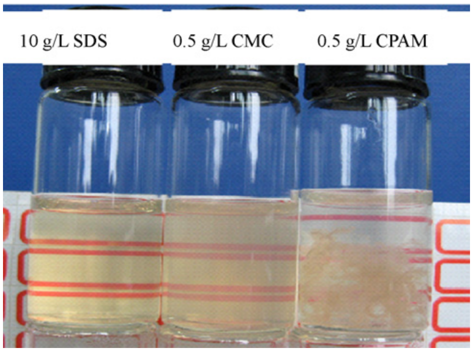

Fig. 7. Colloidal stability of CNC in organic electrolyte solutions.

entanglement resulted in the serious aggregation of CNC. Therefore, low-molecular-weight anionic electrolyte facilitates the stability of negatively charged CNC particles, whereas low-molecular-weight anionic and cation electrolytes will lead to an instable suspension of CNC in aqueous system.

3.3. *Influence of pH on the colloidal stability of CNC suspension*

It was observed in Fig. 8 that as the pH increased from 2 to 11, there were little differences in size and zeta potential among these CNC suspensions. When pH further increased to 12, zeta potential became less negative (−27.8 mV) and size increased to 145 nm. Since sulfate groups are strong anions, it mainly presents in the form of $—O—SO_3—$, instead of $—O—SO_3H_2$ at the pH range of 2–11 (Piai, Rubira, & Muniz, 2009), therefore CNC particles can retain their zeta potential and showed little differences in size and zeta potential at ionic strength of 1 mM. However, the Na^+ concentration at pH 12 was 10 mM, which started to cause particle aggregation (Fig. 3a), and thus the size of CNC increased. Therefore, CNC can be well dispersed in aqueous solution over the pH range of 2–11.

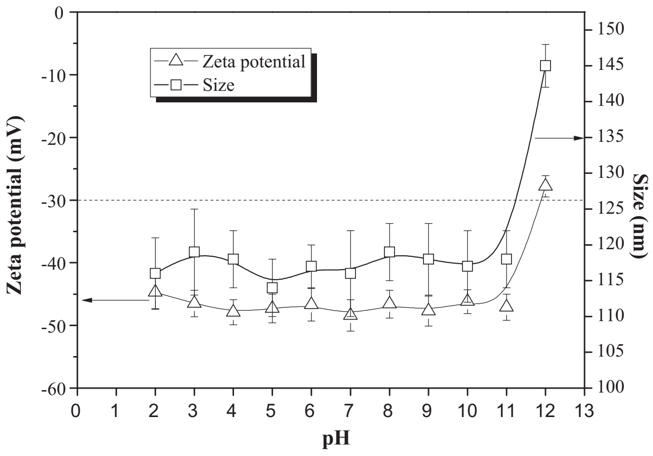

Fig. 8. Zeta potential and size of CNC as a function of pH.

4. Conclusion

Electronegative CNC particles were electrolyte-sensitive in aqueous system; both inorganic and organic electrolytes could affect their colloidal stability. The addition of counterions (Na^+ and Ca^{2+}) resulted in CNC being less negative due to the electrostatic screening effect. The divalent ion Ca^{2+} showed more prominent influence on the colloidal stability of CNC suspension than monovalent Na^+, which was attributed to the stronger screening effect and specific adsorption of Ca^{2+} on the CNC surface. However, the zeta potential of CNC became more negative in anion electrolyte solutions (SDS and CMC). The particle size slightly decreased as SDS concentration increased, whereas serious aggregation occurred to CNC in CMC solution. Strong absorption of cation polyelectrolyte (CPAM) on the electronegative CNC surface and intermolecular interaction among CPAM chains caused CNC aggregation. There were little differences in size and zeta potential among CNC particles at the pH range of 2–11.

Acknowledgments

This work was supported by Financial support from the National Natural Science Foundation of China (No. 31170549) and Ph.D. Programs Foundation of Ministry of Education of China (No. 20090172110022).

References

Araki, J., & Kuga, S. (2001). Steric stabilization of a cellulose microcrystal suspension by poly(ethylene glycol) grafting. *Langmuir*, *17*, 4493–4496.

Beck-Candanedo, S., Roman, M., & Gray, D. G. (2005). *Biomacromolecules*, *6*, 1048–1054.

Beck-Candanedo, S., Viet, D., & Gray, D. G. (2006). Induced phase separation in cellulose nanocrystal suspensions containing ionic dye species. *Cellulose*, *13*, 629–635.

Boluk, Y., Lahiji, R., Zhao, L., & McDermott, M. T. (2011). Suspension viscosities and shape parameter of cellulose nanocrystals (CNC). *Colloids and Surfaces A: Physicochemical and Engineering Aspects*, *377*, 297–303.

Borgström, J., Egermayer, M., Sparrman, T., Quist, P. O., & Piculell, L. (1998). Liquid crystallinity versus gelation of k-carrageenan in mixed salts: Effects of molecular weight, salt composition, and ionic strength. *Langmuir*, *14*, 4935–4944.

Brant, J., Lecoanet, H., Hotze, M., & Wiesner, M. (2005). Comparison of electrokinetic properties of colloidal fullerenes (n-C60) formed using two procedures. *Environmental Science and Technology*, *39*, 6343–6351.

Cranston, E. D., & Gray, D. G. (2006). Morphological and optical characterization of polyelectrolyte multilayers incorporating nanocrystalline cellulose. *Biomacromolecules*, *7*, 2522–2530.

De Souza Lima, M. M., & Borsali, R. (2002). Static and dynamic light scattering from polyelectrolyte microcrystal cellulose. *Langmuir*, *18*, 992–996.

De Souza Lima, M. M., & Borsali, R. (2004). Rodlike cellulose microcrystals: Structure, properties, and applications. *Macromolecular Rapid Communications*, *25*, 771–787.

Dong, X. M., & Gray, D. G. (1997). Effect of counterions on ordered phase formation in suspensions of charged rodlike cellulose crystallites. *Langmuir*, *13*, 2404–2409.

Dong, X. M., Kimura, T., Revol, J. F., & Gray, D. G. (1996). Effects of ionic strength on the isotropic-chiral nematic phase transition of suspensions of cellulose crystallites. *Langmuir*, *12*, 2076–2082.

Dong, X. M., Revol, J. F., & Gray, D. G. (1998). Effect of microcrystallite preparation conditions on the formation of colloid crystals of cellulose. *Cellulose*, *5*, 19–32.

Edgar, C. D., & Gray, D. G. (2002). Influence of dextran on the phase behaviour of suspensions of cellulose nanocrystals. *Macromolecules*, *35*, 7400–7406.

Elazzouzi-Hafraoui, S., Nishiyama, Y., Putaux, J. L., Heux, L., Dubreui, F., & Rochas, C. (2008). The shape and size distribution of crystalline nanoparticles prepared by acid hydrolysis of native cellulose. *Biomacromolecules*, *9*, 57–65.

George, J., & Bawa, A. S. (2010). Synthesis and characterization of bacterial cellulose nanocrystals and their PVA nanocomposites. *Advanced Materials Research*, *123–125*, 383–386.

Habibi, Y., Lucia, L. A., & Rojas, O. J. (2010). Cellulose nanocrystals: Chemistry, self-assembly, and applications. *Chemical Reviews*, *110*, 3479–3500.

Hirai, A., Inui, O., Horii, F., & Tsuji, M. (2009). Phase separation behavior in aqueous suspensions of bacterial cellulose nanocrystals prepared by sulfuric acid treatment. *Langmuir*, *25*, 497–502.

Leong, Y. K., & Ong, B. C. (2003). Critical zeta potential and the Hamaker constant of oxides in water. *Powder Technology*, *134*, 249–254.

Ljungberg, N., Bonini, C., Bortolussi, F., Boisson, C., Heux, L., & Cavaillé, J. Y. (2005). New nanocomposite materials reinforced with cellulose whiskers in atactic polypropylene: Effect of surface and dispersion characteristics. *Biomacromolecules*, *6*, 2732–2739.

Piai, J. F., Rubira, A. F., & Muniz, E. C. (2009). Self-assembly of a swollen chitosan/chondroitin sulfate hydrogel by outward diffusion of the chondroitin sulfate chains. *Acta Biomaterialia*, *5*, 2601–2609.

Revol, J. F., Bradford, H., Giasson, J., Marchessault, R. H., & Gray, D. G. (1992). Helicoidal self-ordering of cellulose microfibrils in aqueous suspension. *International Journal of Biological Macromolecules*, *14*, 170–172.

Samir, M. A. S. A., Alloin, F., & Dufresne, A. (2005). Review of recent research into cellulosic whiskers, their properties and their application in nanocomposite field. *Biomacromolecules*, *6*, 612–626.

Shopsowitz, K. E., Qi, H., Hamad, W. Y., & MacLachlan, M. J. (2010). Free-standing mesoporous silica films with tunable chiral nematic structures. *Nature*, *468*, 422–426.

Sturcova, A., Davies, G. R., & Eichhorn, S. J. (2005). Elastic modulus and stress-transfer properties of tunicate cellulose whiskers. *Biomacromolecules*, *6*, 1055–1061.

Wang, S. C., & Wei, W. C. (2001). Electrokinetic properties of nanosized SiC particles in highly concentrated electrolyte solutions. *Journal of the American Ceramic Society*, *84*, 1411–1414.